

PHYSICAL REVIEW D **89**, 054038 (2014)**Probing the nature of $Y(4260)$ in the isospin violating process $Y(4260) \rightarrow J/\psi\eta\pi^0$** Xiao-Gang Wu,^{1,2,*} Christoph Hanhart,^{2,†} Qian Wang,^{2,‡} and Qiang Zhao^{1,§}¹*Institute of High Energy Physics and Theoretical Physics Center for Science Facilities, Chinese Academy of Sciences, Beijing 100049, China*²*Institut für Kernphysik, Institute for Advanced Simulation, and Jülich Center for Hadron Physics, D-52425 Jülich, Germany*

(Received 30 December 2013; published 31 March 2014)

The isospin violation process $Y(4260) \rightarrow J/\psi\eta\pi^0$ is studied assuming that $Y(4260)$ is a $D_1\bar{D} + c.c.$ hadronic molecule. In association with the production of the $Z_c(3900)$, which is treated as a $D\bar{D}^* + c.c.$ hadronic molecule, this process can help us distinguish the molecular nature of $Y(4260)$ from other scenarios since the incomplete cancellation between the charged and neutral-meson loops, which are prominent in the molecular picture only, produces a peak in the $e^+e^- \rightarrow Y(4260) \rightarrow J/\psi\eta\pi^0$ cross section at the $D_1\bar{D} + c.c.$ threshold and a very prominent peak in the $J/\psi\eta$ invariant mass spectrum in between the $D\bar{D}^* + c.c.$ thresholds, the latter being much narrower than the corresponding one in the isospin conserving channel, i.e. $J/\psi\pi^+\pi^-$. The partial width of $Y(4260) \rightarrow J/\psi\eta\pi^0$ is about 4×10^{-4} times that of $Y(4260) \rightarrow J/\psi\pi^+\pi^-$. The cross section of $e^+e^- \rightarrow Y(4260) \rightarrow J/\psi\eta\pi^0$ at the $D_1\bar{D} + c.c.$ threshold is about 0.05 pb, which is much larger than that produced by the nearby resonances. These features are the direct consequence of the assumed nature of these two states, especially for the $Y(4260)$, which might be accessible at high-statistics experiments such as BESIII and LHCb.

DOI: [10.1103/PhysRevD.89.054038](https://doi.org/10.1103/PhysRevD.89.054038)

PACS numbers: 14.40.Rt, 13.20.Gd, 13.75.Lb

I. INTRODUCTION

Early 2013, the BESIII Collaboration reported a new charged charmoniumlike structure $Z_c(3900)^\pm$ in the $J/\psi\pi^\pm$ invariant mass spectrum in the reaction of $Y(4260) \rightarrow J/\psi\pi^+\pi^-$ [1]. This result was soon confirmed by the Belle Collaboration [2] and in an analysis based on data from the CLEO-c experiment [3]. In addition, Ref. [3] also reported the neutral $Z_c^0(3900)$ at a 3σ significance level in $e^+e^- \rightarrow J/\psi\pi^0\pi^0$ at $\sqrt{s} = 4170$ MeV. These observations immediately initiated many theoretical studies of the $Z_c(3900)$ based on different scenarios such as hadronic molecule [4–6], tetraquark [7], hadro-charmonium [8] and threshold effects [4,9].

The pole of the $Z_c(3900)$ is located near the $D\bar{D}^*$ thresholds and the $Y(4260)$ is near the S -wave $D_1\bar{D}$ thresholds. It was proposed that the $Y(4260)$ and the $Z_c(3900)$ could have sizable $D_1\bar{D}$ and $D\bar{D}^*$ components, respectively [4]. In this scenario the $Y(4260)$ first couples to $D_1\bar{D}$ in an S wave followed by the D_1 decay to $D^*\pi$ in a D wave. Then the strong interactions between the low momentum D and \bar{D}^* will produce the $Z_c(3900)$ near threshold. In Ref. [4], based on the above picture, the invariant mass spectra of $Y(4260) \rightarrow J/\psi\pi^+\pi^-$ were

analyzed, where contributions from both the triangle diagrams with an explicit $Z_c(3900)$ pole and box diagrams without the pole were considered. It turned out that both contributions are needed to reproduce the $J/\psi\pi^+$ and $\pi^+\pi^-$ mass spectra with a clear dominance of the box diagrams. Besides this explanation, various other suggestions exist for the nature of $Y(4260)$, such as the conventional 4S charmonium state [10], the hadro-charmonium state [11–13], the hybrid state [14–16], the $\chi_{c0}\omega$ molecule state [17] and the tetraquark state [18]. In order to further constrain the reaction dynamics and gain deeper insights into the nature of both $Y(4260)$ and $Z_c(3900)$, in this work we propose to investigate the isospin violating process $Y(4260) \rightarrow J/\psi\eta\pi^0$. We will show that the incomplete cancellation between the charged and neutral charmed-meson loops can produce a peak in the $e^+e^- \rightarrow Y(4260) \rightarrow J/\psi\eta\pi^0$ cross section at the $D_1\bar{D}$ threshold and a very narrow peak in the $J/\psi\eta$ invariant mass spectrum at the $D\bar{D}^*$ threshold, which is much more significant and narrower than that in the isospin conserving channel, i.e. $J/\psi\pi^0\pi^0$, since the width is given by the distance of the charged to neutral $D\bar{D}^*$ thresholds. We argue that these are distinct features of the molecular scenario.

The study of the isospin violation process has several benefits. First, the isospin violation process is usually clean compared to the isospin conserved process. The background is reduced significantly, which will make it much easier to identify an isospin violating structure. For instance, in Ref. [19] it has been shown that the open charm effects may be easily identified in the isospin violation

*wuxiaogang@ihep.ac.cn

†c.hanhart@fz-juelich.de

‡q.wang@fz-juelich.de

§zhaoq@ihep.ac.cn

¹We implicitly include the charge conjugation state here and below. The case is the same for $D_1\bar{D}$.

process $e^+e^- \rightarrow (c\bar{c})_{1--} \rightarrow J/\psi\pi^0$, in contrast to those in the isospin conserved processes $e^+e^- \rightarrow J/\psi\eta, \phi\eta_c$. Thus, we expect that the background in $Y(4260) \rightarrow J/\psi\eta\pi^0$ is simpler than that in $Y(4260) \rightarrow J/\psi\pi^+\pi^-$. Second, the isospin violation process may be enhanced by loop effects, especially when molecular structures are involved. As an example, BESIII recently reported the anomalously large isospin violations in $J/\psi \rightarrow \gamma\eta(1405/1475) \rightarrow \gamma 3\pi$ [20]. This phenomenon was explained later by a triangle singularity mechanism [21–23]. It shows that the hadron loops may cause larger isospin violation effects than the direct mixing in threshold production processes. Another example is the very narrow structure observed in $J/\psi \rightarrow \phi\pi^0\eta$ [24] predicted to occur by Refs. [25,26]. Here the width of the structure is determined by the distance between the charged and neutral kaon pair thresholds which enters via the kaon loops. It is also worth mentioning the study of the hadronic width of the $D_{s0}^*(2317)$ in this context. In Refs. [27–29], it was shown that due to the same interplay of loop contributions, the hadronic width of the $D_{s0}^*(2317)$ from its isospin violating decay to $\pi^0 D_s$ gets enhanced significantly, if the $D_{s0}^*(2317)$ is a DK molecule. This is exactly analogous to the mechanisms at work in this paper. On the other hand, the structure would have been much broader if any other mechanism besides the kaon loops (for instance, the $\pi^0 - \eta$ mixing) had been dominant. Thus, in this work we study the effect of both the heavy meson loops and $\pi^0 - \eta$ mixing. Third, in the charmonium energy region, we have several high-statistics and high-luminosity machines feeding experiments such as BESIII, Belle, BABAR and LHCb. It is very promising that the isospin violation process $Y(4260) \rightarrow J/\psi\eta\pi^0$ can be accessible at one of these facilities.

This work is organized as follows: We illustrate our framework in Sec. II. The results and discussions are presented in Sec. III, and a summary is given in the last section.

II. FRAMEWORK

A. Feynman diagrams

Our calculation is based on the assumption that the $Y(4260)$ is dominated by $D_1\bar{D}$ and that $Z_c(3900)$ is dominated by $D\bar{D}^*$. The relevant Feynman diagrams for $Y(4260) \rightarrow J/\psi\eta\pi^0$ are listed in Fig. 1, where Fig. 1(a) represents the triangle diagrams through an intermediate $Z_c(3900)$ and Figs. 1(b), 1(c), and 1(d) are box diagrams which are similar to those in Ref. [4] for the isospin conserving process $Y(4260) \rightarrow J/\psi\pi^0\pi^0$. Apart from these contributions, we also consider the contribution from $\pi^0 - \eta$ mixing as shown in Fig. 2. The gray square means that all the possible diagrams of $Y(4260) \rightarrow J/\psi\pi^0\pi^0$ as in Ref. [4] are included, and the black circle is the mixing between π^0 and η . The mixing intensity can be determined by

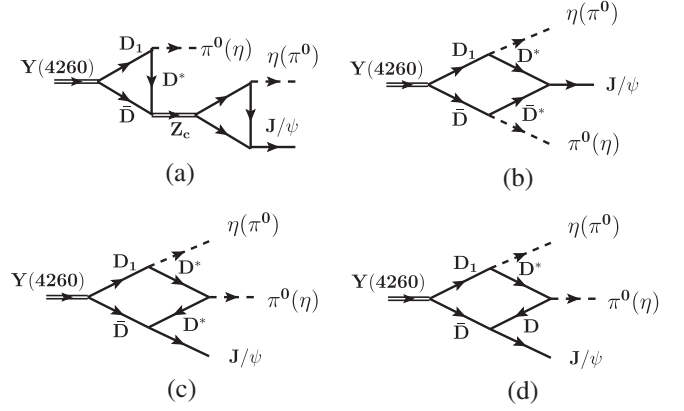


FIG. 1. Feynman diagrams for $Y(4260) \rightarrow J/\psi\eta\pi^0$, which are classified as: (a) Triangle diagrams with the explicit $Z_c(3900)$ pole; (b–d) Box diagrams without the pole.

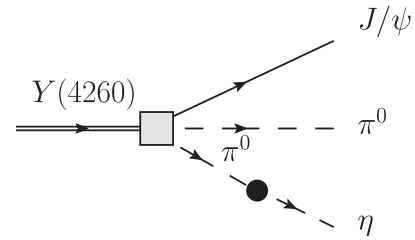


FIG. 2. The schematic diagram for the π^0 - η mixing. The square denotes that all the allowed diagrams in Fig. 1 contributing to $Y(4260) \rightarrow J/\psi\pi^0\pi^0$ are included, and the round dot represents the mixing between π^0 and η .

$$\epsilon_0 = \frac{1}{\sqrt{3}} \frac{M_{K^0}^2 - M_{K^+}^2 + M_{\pi^+}^2 - M_{\pi^0}^2}{M_\eta^2 - M_{\pi^0}^2} = 0.01 \quad (1)$$

using Dashen's theorem [30].

B. Effective Lagrangians

The diagrams in our framework are described by the nonrelativistic effective field theory (NREFT) introduced in Refs. [31,32] in which the heavy fields are treated nonrelativistically while the light mesons, π and η , are treated relativistically.

Although the related Lagrangians and couplings in this paper can be found in Refs. [4,33], we list some of them for completeness. By assuming $Y(4260)$ is an S -wave $D_1\bar{D}$ molecular state with $I^G(J^{PC}) = 0^-(1^{--})$, the Lagrangian for its coupling to the constituents reads [4,33]

$$\mathcal{L}_Y = \frac{y}{\sqrt{2}} Y^{i\dagger} (D_{1a}^i \bar{D}_a - D_a \bar{D}_{1a}^i) + \text{H.c.}, \quad (2)$$

where $Y^{i\dagger}$ is the creation operator for $Y(4260)$ and the other operators denote the annihilation operators for the corresponding particles. The renormalized effective coupling y is related to the probability of finding the $D_1\bar{D}$ component

in the physical wave function of $Y(4260)$, which can be estimated from Weinberg's compositeness theorem [34,35]. Based on these considerations $|y| = 3.28 \pm 1.4 \text{ GeV}^{-1/2}$ is extracted in Refs. [4,33]. However, all results shown here are insensitive to the value of y , since the overall normalization of the predicted rates is fixed by the measured $e^+e^- \rightarrow J/\psi\pi\pi$ cross section.

The newly discovered $Z_c(3900)$ [1–3] is a charged charmoniumlike state with $I^G(J^{PC}) = 1^+(1^{+-})$ for its charge-neutral state, which is the charm sector's analogue of Z_b . If $Z_c(3900)$ is an S -wave $D\bar{D}^*$ molecular state, the interaction Lagrangian reads [36]

$$\mathcal{L}_Z = z(\bar{V}^{\dagger i} Z^i P^{\dagger} - \bar{P}^{\dagger} Z^i V^{\dagger i}) + \text{H.c.} \quad (3)$$

The $Z_c(3900)$ isotriplet can be written as a 2×2 matrix

$$Z_{ba} = \begin{pmatrix} \frac{1}{\sqrt{2}} Z^0 & Z^+ \\ Z^- & -\frac{1}{\sqrt{2}} Z^0 \end{pmatrix}_{ba}, \quad (4)$$

and the charmed mesons are given by $P(V) = (D^{(*)0}, D^{(*)+})$. Current data do not allow one to decide if the S -matrix singularity related to the $Z_c(3900)$ is located above or below the $D\bar{D}^*$ threshold, and thus we cannot calculate the parameter z analogously to what was done in the case of the $Y(4260)$. Phenomenologically, however, we can get this coupling constant from an analysis of the data for $Y(4260) \rightarrow J/\psi\pi^+\pi^-$. The analysis of Ref. [4] revealed

$$|z| = (0.77 \pm 0.23) \text{ GeV}^{-1/2}. \quad (5)$$

To incorporate the η meson, we adopt the pseudoscalar octet

$$\phi = \begin{pmatrix} \frac{1}{\sqrt{2}}\pi^0 + \frac{1}{\sqrt{6}}\eta & \pi^- & K^+ \\ \pi^- & -\frac{1}{\sqrt{2}}\pi^0 + \frac{1}{\sqrt{6}}\eta & K^0 \\ K^- & \bar{K}^0 & -\frac{2}{\sqrt{6}}\eta \end{pmatrix}, \quad (6)$$

where we have identified the η meson as the SU(3) octet element η_8 . In the heavy quark limit, the heavy and light degrees of freedom are conserved separately. So the heavy mesons can be classified by their light degrees of freedom, i.e., $s_l = s_q + l$ with s_q the spin of the light quark and l the orbital angular momentum. The narrow P -wave meson D_1 is considered as a $s_l = 3/2$ state and decays to $D^*\pi$ in a D wave. The interaction Lagrangian reads [37]

$$\begin{aligned} \mathcal{L}_{D_1} = & i \frac{h'}{f_\pi} [3D_{1a}^i (\partial^i \partial^j \phi_{ab}) D_b^{*j} - D_{1a}^i (\partial^j \partial^i \phi_{ab}) D_b^{*j}] \\ & + 3\bar{D}_a^{*i} (\partial^i \partial^j \phi_{ab}) \bar{D}_{1b}^j - \bar{D}_a^{*i} (\partial^j \partial^i \phi_{ab}) \bar{D}_{1b}^j] + \text{H.c.} \end{aligned}$$

From the width of D_1 , the coupling h' is determined to be $|h'| = (0.62 \pm 0.08) \text{ GeV}^{-1}$ [38].

C. $e^+e^- \rightarrow Y(4260) \rightarrow J/\psi\eta\pi^0$ and the propagator of $Y(4260)$

The cross section of e^+e^- annihilation to any final states via a vector meson can be expressed by the vector meson dominance via the effective photon-vector-meson coupling g_{γ^*V} (see e.g. [39]). For the full process $e^+e^- \rightarrow Y(4260) \rightarrow J/\psi\eta\pi^0$, this yields

$$\sigma(s) = (4\pi\alpha)^2 \left(g_{\gamma^*Y} \frac{M_Y^2}{s} \right)^2 (M_Y \Gamma_{Y \rightarrow J/\psi\eta\pi^0}) |G_Y(s)|^2 \quad (7)$$

where g_{γ^*Y} is the dimensionless coupling constant between the virtual photon and vector state $Y(4260)$, and $G_Y(s)$ is the propagator of $Y(4260)$, i.e. [36]

$$G_Y^{-1} = s - M_Y^2 + \hat{\Pi}(s) + iM_Y\Gamma_Y \quad (8)$$

with

$$\hat{\Pi}(s) = \Pi(s) - \text{Re}[\Pi(M_Y^2) + (s - M_Y^2)\partial_s \Pi(s)|_{s=M_Y^2}]. \quad (9)$$

In the above equation, the self-energy $\hat{\Pi}(s)$ is doubly subtracted at mass position $M_Y = (4220 \pm 5) \text{ MeV}$ which is fitted by the data for $e^+e^- \rightarrow Y(4260) \rightarrow J/\psi\pi^+\pi^-$ and $h_c\pi^+\pi^-$ [38]. Here $\Pi(s)$ is the $D_1\bar{D}$ bubble diagram contributing to the $Y(4260)$ self-energy. $\Gamma_Y = (40 \pm 9) \text{ MeV}$ is the constant partial decay width of the $Y(4260)$ without going through the $D_1\bar{D}$ component, namely, the non- $D_1\bar{D}$ decay width [38].

III. RESULTS AND DISCUSSION

A. $J/\psi\eta$, $J/\psi\pi^0$ and $\eta\pi^0$ invariant mass distributions

In Fig. 3 the numerical results for $Y(4260) \rightarrow J/\psi\eta\pi^0$ are presented, where the invariant mass spectra for the final state, $J/\psi\eta$, $J/\psi\pi^0$ and $\eta\pi^0$, are plotted for each mechanism individually. Since there are still large uncertainties with the coupling between $Y(4260)$ and $D_1\bar{D}$, it is more convenient to define the ratio of the partial width of $Y(4260) \rightarrow J/\psi\eta\pi^0$ to $\Gamma_{Y(4260) \rightarrow J/\psi\pi^+\pi^-}$, in which case the coupling uncertainties cancel. As shown by the left column of Fig. 3, i.e. (a), (d), (g), and (j), a peak around 3.9 GeV appears in the invariant mass spectrum of $J/\psi\eta$ in all the cases. However, the line shapes, as well as the predicted rates, are quite different from each other: The peaks from the triangle [Fig. 3(a)] and box diagrams [Fig. 3(d)] are located at the $D\bar{D}^*$ thresholds with a narrow width of about 8 MeV reflecting the mass difference between the charged and neutral $D\bar{D}^*$ thresholds. In addition, in these cases the peaks are asymmetric, and the asymmetry is most pronounced in Fig. 3(a) where the $Z_c(3900)$ pole contributes. However, since the contribution of the box diagrams is much larger than that of the $Z_c(3900)$, we cannot pin down the molecular nature of the $Z_c(3900)$ just from the small asymmetric effect.

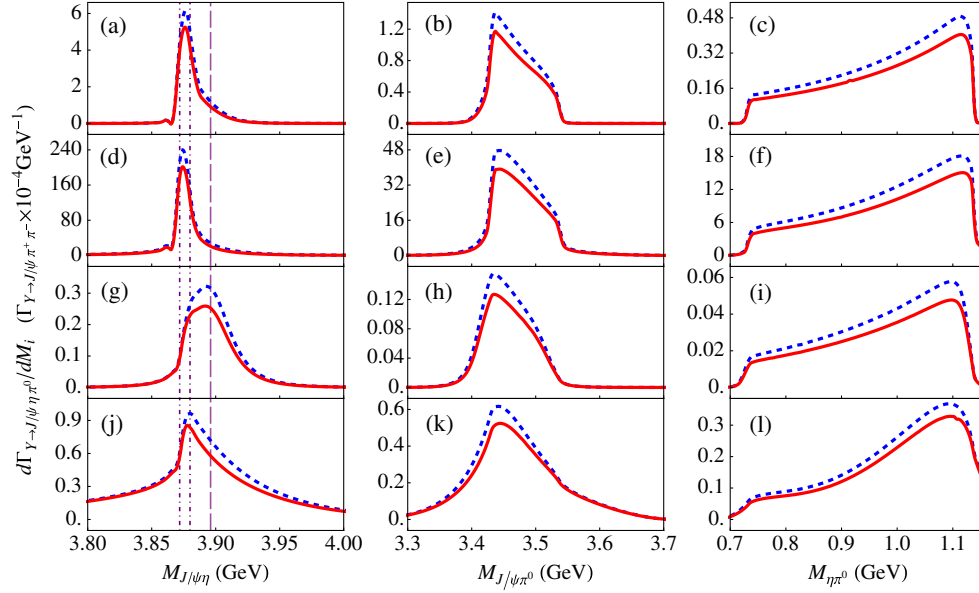


FIG. 3 (color online). The invariant mass spectra for the final state $J/\psi\eta$ (left column), $J/\psi\pi^0$ (middle column), and $\eta\pi^0$ (right column) in $Y(4260) \rightarrow J/\psi\eta\pi^0$ evaluated for a total energy of 4260 MeV. Figures (a–c) in the first row are the contributions from the triangle diagrams, Figures (d–f) in the second row are for the box diagrams, Figures (g–i) in the third row are for the π^0 - η mixing through triangle diagrams, and Figures (j–l) in the fourth row are for the π^0 - η mixing through box diagrams. The solid (red) and dashed (blue) lines stand for the contributions with and without considering the width of D_1 . The three vertical lines in the left column denote the $D^0\bar{D}^{*0}$ and $D^+\bar{D}^{*-}$ threshold, and the $Z_c(3900)$ mass, respectively. All the differential partial widths have been normalized to the partial width of the isospin conserving process, i.e. $\Gamma_{Y(4260) \rightarrow J/\psi\pi^+\pi^-}$.

The reason for the appearance of this narrow structure is that the charged and neutral meson loops interfere destructively in isospin violating transitions, since these two amplitudes have to cancel in the absence of the $D(D^*)$ meson mass differences. In effect, the leading isospin violating contribution comes from the difference of the two-meson cut contributions of the individual amplitudes which is proportional to the phase space and its analytic continuation to below threshold in the neutral and charged channels, respectively. This contribution is nonanalytic in the quark masses and can lead to significantly enhanced violating effects; namely, the sum of amplitudes driven by the meson mass differences will outnumber those from $\pi^0 - \eta$ mixing by 1 order of magnitude. The same mechanism is also responsible for the isospin violation decay $\eta(1405) \rightarrow 3\pi$ [21,22] and $a_0 - f_0$ mixing in $J/\psi \rightarrow \phi\pi^0\eta$ [25,26]. For those two cases, since their decay mechanism is through the kaon loops, a similar peak near the $K\bar{K}^{(*)}$ threshold has been found in $\pi\pi$ and $\eta\pi^0$ invariant mass spectra. This shows that the dominant isospin violating process is sensitive to the significance of the intermediate two-meson states in the wave functions of the relevant hadron. In this sense it provides a direct measure of the molecular component of the states.

On the other hand, the spectra from any mechanism that is not driven by the mass differences of the open charm mesons in the loops are expected to be significantly broader and more similar to the isospin conserving counterparts. For illustration, in Figs. 3(g) and 3(j) we show the spectra

that emerge, if the isospin violation comes from π^0 - η mixing. The reason is that here the transition matrix element is the same as its isospin conserving counterparts since the isospin violation occurs only on one of the external pion legs. In particular, in these two cases the loops interfere constructively.

For the $J/\psi\pi^0$ spectrum, there is a broad bump near 3.4–3.5 GeV in all four mechanisms, as shown in the middle column of Fig. 3, i.e. Figs. 3(b), 3(e), 3(h), and 3(k), which is the kinematical reflection of the narrow peak in the $J/\psi\eta$ spectrum. The line shape of the $\eta\pi^0$ spectrum is very similar to the $\pi^+\pi^-$ spectrum investigated in $Y(4260) \rightarrow J/\psi\pi^+\pi^-$ before considering the final state interactions. The structures near 0.73 and 1.13 GeV are also the kinematical reflections of the peak in the $J/\psi\eta$ spectrum [4].

For the $J/\psi\pi^+\pi^-$ channel, the BESIII data [1] provide a constraint on the ratio between the triangle and box diagrams [4],²

$$\frac{\Gamma(Y(4260) \rightarrow J/\psi\pi^+\pi^-)_{\text{triangle}}}{\Gamma(Y(4260) \rightarrow J/\psi\pi^+\pi^-)_{\text{box}}} \approx 12\%. \quad (10)$$

In the case of isospin violation, the dominance of the box diagram is even larger: The analogous ratio to Eq. (10) here gives 2%. In order to better understand how the isospin

²Here we do not consider the $\pi\pi$ final state interaction which in the scenario discussed here only gives a small correction since the pions are predominantly in a D wave.

violation works quantitatively for each mechanism individually, we define the ratio

$$\xi_m \equiv \frac{\Gamma(Y(4260) \rightarrow J/\psi\eta\pi^0)_m}{\Gamma(Y(4260) \rightarrow J/\psi\pi^+\pi^-)_m}, \quad (11)$$

where the subscript represents the specific mechanism. It should be stressed that the values of the ratio ξ_m cannot be compared directly to observables since the quantity in the denominator provides, in general, only a small fraction of the cross section.

One finds that the box contribution with the isospin violation driven by the meson mass differences in the loop provides the largest effect, i.e. $\xi_{\text{box}} = 4 \times 10^{-4}$. In contrast, the triangle diagrams give, in connection with the same mechanism, $\xi_{\text{triangle}} = 1 \times 10^{-4}$. The reason for this difference is that the contribution from $Y(4260) \rightarrow Z_c^0\pi^0 \rightarrow (J/\psi\eta)\pi^0$ is much larger than that from $Y(4260) \rightarrow Z_c^0\eta \rightarrow (J/\psi\pi^0)\eta$ since the first triangle loop of the former process satisfies the triangle singularity condition [21,22,40], while the latter process does not.

On the other hand, the two ratios for the diagrams where the isospin violation is modeled by the π^0 - η mixing are of similar size, about 1×10^{-5} , but a factor of 40 smaller than the leading ratio ξ_{box} . The size of these ratios can be understood quantitatively since the isospin violation can be estimated via the difference in phase spaces

$$\xi_{\text{mixing}} = |\epsilon_0|^2 \frac{P.S.(Y(4260) \rightarrow J/\psi\eta\pi^0)}{P.S.(Y(4260) \rightarrow J/\psi\pi^+\pi^-)} = 3.52 \times 10^{-5}. \quad (12)$$

This implies that all mechanisms that are not enhanced by the nonanalytic isospin violating terms from the loops should be similar in size.

As one can see from Fig. 3 the width effects of the D_1 are about 10% for each individual spectrum. The main uncertainty in our calculation comes from the mass difference between the charged and neutral D_1 , for which we have adopted $M_{D_1^+} - M_{D_1^0} = M_{D^{*+}} - M_{D^{*0}}$. If we use an equal mass for the charged and neutral D_1 , the results will change by about 30% in those contributions where the isospin violation was driven by the meson mass differences, while the changes to the mixing diagrams are negligible. This is again because the charged and neutral loops interfere destructively in the former group, while the interference is constructive in the latter.

B. The line shape of $Y(4260)$ in the $e^+e^- \rightarrow Y(4260) \rightarrow J/\psi\eta\pi^0$ process

Using Eq. (7) and the parameters fitted in the $J/\psi\pi^+\pi^-$ and $h_c\pi^+\pi^-$ channels [38], we can predict the cross section for $e^+e^- \rightarrow Y(4260) \rightarrow J/\psi\eta\pi^0$ as a function of the center-of-mass energy, as shown in Fig. 4. Again, because of the destructive interference between the charged and

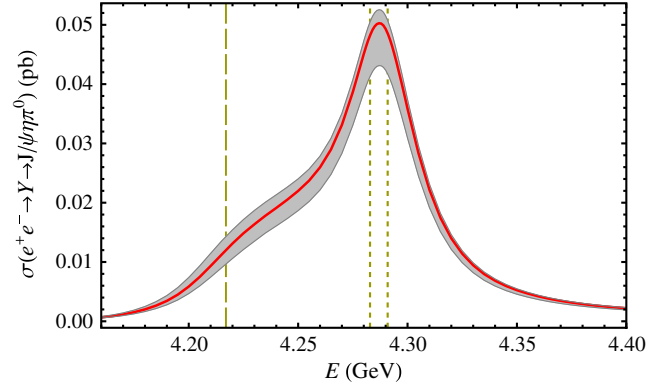


FIG. 4 (color online). The predicted cross section for $e^+e^- \rightarrow Y(4260) \rightarrow J/\psi\eta\pi^0$. The two vertical short-dashed lines denote the charged and neutral $D_1\bar{D}$ thresholds, respectively, while the long-dashed line denotes the location of the $Y(4260)$ pole as it emerged from the fit to the isospin conserving data. The grey band shows the variation of our prediction, when the parameters are allowed to vary within the statistical uncertainty allowed by the fit to the isospin conserving data.

neutral charmed-meson loops in the dominant contributions, the isospin violating cross section is maximal, of order 0.05 pb, close to the charged and neutral $D_1\bar{D}$ thresholds and *not* at the location of the $Y(4260)$ pole. This is a highly nontrivial prediction of the scenario explored in this paper. Contrary to the spectra discussed in the previous subsection, the line shape of $e^+e^- \rightarrow Y(4260) \rightarrow J/\psi\eta\pi^0$ turns out to be very sensitive to the D_1 width because the effect of the $D_1\bar{D}$ cut gets weakened by the fact that the width pushes the corresponding branch point into the complex plane. This results in the width of the structure not being given by the splitting between the charged and neutral $D_1\bar{D}$ thresholds, but by the width of the D_1 . To be more specific, when we switch off the D_1 width in our calculation, the peak at the $D_1\bar{D}$ thresholds gets very narrow, and at the same time, the predicted cross section between the thresholds rises by 1 order of magnitude.

It is interesting to compare the isospin violating mechanisms based on different scenarios. In the tetraquark picture [7,18], the isospin violating effect is included by inserting the explicit effective Lagrangian into the isospin symmetric amplitudes. In the hadro-charmonium picture [11–13], this breaking can only happen through the π^0 - η mixing. Both these scenarios give relatively small cross sections that are proportional to $(m_d - m_u)/m_s$ and especially are not related to the $D_1\bar{D}$ threshold. Meanwhile, if $Y(4260)$ is a $\chi_{c0}\omega$ molecule [17], its main decay mode should be $\chi_{c0} + \omega$ or $\chi_{c0} + 3\pi$, and the corresponding isospin violation decay channels would be $\chi_{c0} + \rho^0$ or $\chi_{c0} + 2\pi$ through ω - ρ mixing. This mixing strength is much smaller than that between π^0 and η . For instance, the recent analysis of Ref. [41] gave a value of -0.002 for the mixing strength. This is a factor of 5 smaller than the value given in Eq. (1). The total strength of the cross section from this

scenario would thus be smaller by a factor of more than 3 orders of magnitude compared to that in the $D_1\bar{D}$ molecule picture. In addition, the $\chi_{c0}\omega$ molecule nature will be sensitive to the $\chi_{c0}\omega$ threshold instead of the $D_1\bar{D}$ threshold. Therefore, a measurement of a $D_1\bar{D}$ threshold enhancement in the isospin violation process would be an unambiguous proof for a prominent $D_1\bar{D}$ molecular nature of $Y(4260)$.

IV. SUMMARY

In this work, we assume that $Y(4260)$ and $Z_c(3900)$ are hadronic molecules composed of $D_1\bar{D}$ and $D\bar{D}^*$, respectively, as in Refs. [4,5,33]. We investigate the isospin violation process $Y(4260) \rightarrow J/\psi\eta\pi^0$ by considering triangle diagrams, box diagrams and π^0 - η mixings. We find that the position and width of the $D\bar{D}^* + c.c.$ threshold peak in the $J/\psi\eta$ invariant mass spectrum depends on the production mechanism. Within the scenario outlined in the paper, we predict a very narrow peak (width below 10 MeV) located between the thresholds for the neutral and charged $D\bar{D}^*$ channels even without the explicit contributions from Z_c . On the other hand, if the Z_c is not a $D\bar{D}^*$ molecule, we would expect a peak with a broader width of about 46 MeV in the $J/\psi\eta$ spectra. The partial width of the $J/\psi\eta\pi^0$ channel is about 4×10^{-4} with

respect to that of the $J/\psi\pi^+\pi^-$ channel. In addition, we predict that, if the $Y(4260)$ is predominantly a $D_1\bar{D}$ molecule, the line shape of $e^+e^- \rightarrow J/\psi\eta\pi^0$ is very different from that in the isospin conserving transition $e^+e^- \rightarrow J/\psi\pi\pi$. In particular, it should peak at the $D_1\bar{D}$ thresholds instead of the pole position of the $Y(4260)$.

It should be stressed that what was assumed in this paper is that the $Y(4260)$ and $Z_c(3900)$ are pure $D_1\bar{D}$ and $D\bar{D}^*$ molecules, respectively. Any admixture of other components in the wave functions would make the peak shown in Fig. 4 smaller. Therefore, future experimental investigations of the peculiar structures predicted in the $J/\psi\eta$ invariant mass near the $D\bar{D}^*$ threshold and the total cross section near the $D_1\bar{D}$ threshold will be important steps towards an understanding of the nature of the $Y(4260)$.

ACKNOWLEDGMENTS

The authors are in debt to Feng-Kun Guo for having benefitted from his ‘‘AmpCalc.m’’ package in our computation. This work is supported, in part, by the National Natural Science Foundation of China (Grants No. 11035006 and No. 11121092), the Chinese Academy of Sciences (KJCX3-SYW-N2), the Ministry of Science and Technology of China (2009CB825200), and DFG and NSFC funds to the Sino-German CRC 110.

-
- [1] M. Ablikim *et al.* (BESIII Collaboration), *Phys. Rev. Lett.* **110**, 252001 (2013).
- [2] Z. Q. Liu *et al.* (Belle Collaboration), *Phys. Rev. Lett.* **110**, 252002 (2013).
- [3] T. Xiao, S. Dobbs, A. Tomaradze, and K. K. Seth, *Phys. Lett. B* **727**, 366 (2013).
- [4] Q. Wang, C. Hanhart, and Q. Zhao, *Phys. Rev. Lett.* **111**, 132003 (2013).
- [5] F.-K. Guo, C. Hidalgo-Duque, J. Nieves, and M. P. Valderrama, *Phys. Rev. D* **88**, 054007 (2013).
- [6] E. Wilbrink, H.-W. Hammer, and U.-G. Meiner, *Phys. Lett. B* **726**, 326 (2013).
- [7] L. Maiani, V. Riquer, R. Faccini, F. Piccinini, A. Pilloni, and A. D. Polosa, *Phys. Rev. D* **87**, 111102 (2013).
- [8] M. B. Voloshin, *Phys. Rev. D* **87**, 091501 (2013).
- [9] D.-Y. Chen, X. Liu, and T. Matsuki, *Phys. Rev. Lett.* **110**, 232001 (2013).
- [10] F. J. Llanes-Estrada, *Phys. Rev. D* **72**, 031503 (2005).
- [11] M. B. Voloshin, *Prog. Part. Nucl. Phys.* **61**, 455 (2008).
- [12] S. Dubynskiy and M. B. Voloshin, *Phys. Lett. B* **666**, 344 (2008).
- [13] X. Li and M. B. Voloshin, *arXiv:1309.1681*.
- [14] S.-L. Zhu, *Phys. Lett. B* **625**, 212 (2005).
- [15] E. Kou and O. Pene, *Phys. Lett. B* **631**, 164 (2005).
- [16] F. E. Close and P. R. Page, *Phys. Lett. B* **628**, 215 (2005).
- [17] L. Y. Dai, M. Shi, G.-Y. Tang, and H. Q. Zheng, *arXiv:1206.6911*.
- [18] L. Maiani, V. Riquer, F. Piccinini, and A. D. Polosa, *Phys. Rev. D* **72**, 031502 (2005).
- [19] Q. Wang, X.-H. Liu, and Q. Zhao, *Phys. Rev. D* **84**, 014007 (2011).
- [20] M. Ablikim *et al.* (BESIII Collaboration), *Phys. Rev. Lett.* **108**, 182001 (2012).
- [21] J.-J. Wu, X.-H. Liu, Q. Zhao, and B.-S. Zou, *Phys. Rev. Lett.* **108**, 081803 (2012).
- [22] X.-G. Wu, J.-J. Wu, Q. Zhao, and B.-S. Zou, *Phys. Rev. D* **87**, 014023 (2013).
- [23] F. Aceti, W. H. Liang, E. Oset, J. J. Wu, and B. S. Zou, *Phys. Rev. D* **86**, 114007 (2012).
- [24] M. Ablikim *et al.* (BES III Collaboration), *Phys. Rev. D* **83**, 032003 (2011).
- [25] J.-J. Wu, Q. Zhao, and B. S. Zou, *Phys. Rev. D* **75**, 114012 (2007).
- [26] C. Hanhart, B. Kubis, and J. R. Pelaez, *Phys. Rev. D* **76**, 074028 (2007).
- [27] A. Faessler, T. Gutsche, V. E. Lyubovitskij, and Y.-L. Ma, *Phys. Rev. D* **76**, 014005 (2007).
- [28] M. F. M. Lutz and M. Soyeur, *Nucl. Phys. A* **813**, 14 (2008).
- [29] F.-K. Guo, C. Hanhart, S. Krewald, and U.-G. Meißner, *Phys. Lett. B* **666**, 251 (2008).
- [30] R. F. Dashen, *Phys. Rev.* **183**, 1245 (1969).

- [31] S. Fleming and T. Mehen, *Phys. Rev. D* **78**, 094019 (2008).
- [32] F.-K. Guo, C. Hanhart, G. Li, U.-G. Meißner, and Q. Zhao, *Phys. Rev. D* **83**, 034013 (2011).
- [33] F.-K. Guo, C. Hanhart, U.-G. Meißner, Q. Wang, and Q. Zhao, *Phys. Lett. B* **725**, 127 (2013).
- [34] S. Weinberg, *Phys. Rev.* **137**, B672 (1965).
- [35] V. Baru, J. Haidenbauer, C. Hanhart, Y. Kalashnikova, and A. E. Kudryavtsev, *Phys. Lett. B* **586**, 53 (2004).
- [36] M. Cleven, Q. Wang, F.-K. Guo, C. Hanhart, U.-G. Meißner, and Q. Zhao, *Phys. Rev. D* **87**, 074006 (2013).
- [37] P. Colangelo, F. De Fazio, and R. Ferrandes, *Phys. Lett. B* **634**, 235 (2006).
- [38] M. Cleven, Q. Wang, F.-K. Guo, C. Hanhart, U.-G. Meißner, and Q. Zhao, [arXiv:1310.2190](https://arxiv.org/abs/1310.2190).
- [39] S. Donnachie, G. Dosch, P. Landshoff, and O. Nachtmann, *Pomeron Physics and QCD* (Cambridge University Press, Cambridge, 2002).
- [40] Q. Wang, C. Hanhart, and Q. Zhao, *Phys. Lett. B* **725**, 106 (2013).
- [41] C. Hanhart, *Phys. Lett. B* **715**, 170 (2012).